Shubhika Shubhika

shubhika

Quick Submit

Quick Submit

Dr. B R Ambedkar National Institute of Technology, Jalandhar

Document Details

Submission ID
trn:oid:::1:3579406073

Submission Date
May 26, 2026, 4:19 PM GMT+5:30

Download Date
May 26, 2026, 4:22 PM GMT+5:30

File Name
thesis_1.docx

File Size
2.8 MB

40 Pages

7,340 Words

46,378 Characters

2% Overall Similarity

The combined total of all matches, including overlapping sources, for each database.

Match Groups

10 Not Cited or Quoted 2%
Matches with neither in-text citation nor quotation marks

0 Missing Quotations 0%
Matches that are still very similar to source material

0 Missing Citation 0%
Matches that have quotation marks, but no in-text citation

0 Cited and Quoted 0%
Matches with in-text citation present, but no quotation marks

Top Sources

1% Internet sources
1% Publications
1% Submitted works (Student Papers)

Integrity Flags

0 Integrity Flags for Review

No suspicious text manipulations found.

Our system's algorithms look deeply at a document for any inconsistencies that would set it apart from a normal submission. If we notice something strange, we flag it for you to review.

A Flag is not necessarily an indicator of a problem. However, we'd recommend you focus your attention there for further review.

Match Groups

- **10** Not Cited or Quoted 2%
  Matches with neither in-text citation nor quotation marks
- **0** Missing Quotations 0%
  Matches that are still very similar to source material
- **0** Missing Citation 0%
  Matches that have quotation marks, but no in-text citation
- **0** Cited and Quoted 0%
  Matches with in-text citation present, but no quotation marks

Top Sources

1% Internet sources
1% Publications
1% Submitted works (Student Papers)

Top Sources

The sources with the highest number of matches within the submission. Overlapping sources will not be displayed.

1	Internet	
www.mdpi.com		<1%
2	Publication	
"Artificial Intelligence: Theory and Applications", Springer Science and Business ...		<1%
3	Student papers	
Ravensbourne		<1%
4	Student papers	
University of Hertfordshire		<1%
5	Student papers	
University of Glasgow		<1%
6	Internet	
garph.co.uk		<1%
7	Internet	
euroasiapub.org		<1%
8	Internet	
ispprt.co.za		<1%
9	Internet	
ijsrem.com		<1%
10	Internet	
travelpackpro.net		<1%

ABSTRACT

This study presents a bio-augmented photovoltaic (PV) system incorporating luminescent compounds extracted from mango and pomegranate peel waste to enhance solar energy conversion under diffuse irradiance conditions. Bioactive chromophores—primarily anthocyanins and flavonoids—were isolated through ethanol-assisted extraction and deposited as an optical down-converting layer on glass substrates interfaced with silicon wafers. UV–Vis spectroscopy revealed characteristic absorbance peaks at 320, 420, 540, and 740 nm, confirming the presence of UV-A and visible light–responsive luminophores capable of photon re-emission. FTIR analysis indicated the retention of functional phenolic groups essential for fluorescence activity. Performance assessment demonstrated that the bio-based panel achieved higher voltage output than a conventional PV module under both direct sunlight (5.8 V vs. 5.2 V) and UV illumination (3.8 V vs. 2.2 V). Temperature–voltage characterization showed reduced thermal sensitivity, with the bio-panel maintaining improved stability across 25–45°C, indicating mitigation of thermal degradation due to spectral conversion and moderated heat absorption. The results validate the functional capability of biodegradable luminescent films to enhance PV performance while enabling waste valorization and sustainability. Future integration with IoT-enabled sensors and AI-driven diagnostics will facilitate adaptive optimization and predictive performance modelling for distributed solar energy systems.

CHAPTER 1

1. INTRODUCTION

The demand of energy is rapidly changing in global context towards renewable, sustainable and decentralized power supply systems. They are primarily driven due to increase in concerns over huge climate change, exhaustion of non-renewable resources, and the alarming need for reducing carbon footprints [1]. Solar photovoltaic (PV) systems have emerged as one of the most important contributors to this drastic energy shift [2]. India has appeared as one of the world's fastest developing solar energy markets, directed by national missions such as the Jawaharlal Nehru National Solar Mission (JNNSM) and the extensive target of achieving around 500 GW of renewable energy capacity by 2030[3]. Since 2024, India's positioned solar capacity has transcend 82 GW, with rapid extension in majorly utility projects, rooftop networks, and decentralized micro grids in Indian villages [4].

Conventional silicon-based solar modules continue to counter several limitations in context of efficiency, sustainability, operational issues, adaptability, and end waste management. These obstructions are especially profound in regions with high differentiable climatic conditions such as dark cloudy, shaded, or significantly low-irradiance environments [5]. However, the efficiency losses in presence of diffuse light remain a critical constriction for expanding solar acceptance in geographically diverse and metropolitan areas. Also, the manufacturing of PV modules involves energy rigorous processes and the use of hazardous heavy metal materials as components such as lead, cadmium, mercury, chromium, arsenic etc[6]. As these conventional panels reach their 20–25 year operational lifespan, inappropriate disposal poses highly significant environmental risks majorly leaching of these heavy metals directly into soil as well as water bodies, contributing substantially towards greater environmental pollution concerns [7]. These challenges have promoted a serious global push to thrive an alternative solar materials that are both functionally more efficient and environmentally favorable.

Simultaneously, large amount of fruit-processing waste persist neglected in India, despite having high-value bioactive compounds with distinctive optical properties [8] . Pomegranate and mango peels, in specific, are rich in secondary metabolites like anthocyanin, carotenoids, flavonoids, phenolic compounds and other phytochemical constituents that are known to demonstrate significant luminescent behavior through fluorescence, energy emission transition and light-scattering phenomena [9]. Therefore, harnessing bio-derived luminescent compounds formulate thus a low-cost, biodegradable, optically active and functionally sustainable materials capable of uplifting solar energy capture specially under non-ideal lighting environment [10] .

1.1 OVERVIEW – ROLE OF ARTIFICIAL INTELLIGENCE

Artificial intelligence (AI) assisted monitoring have gained much attention in current years globally because of their potential to analyze real-time datasets. Recent research in photovoltaic systems increasingly utilize machine-learning to improve energy monitoring, and control regulations [11]. Applied deep-learning models like CNN-LSTM hybrid in AI-solar module, reported 35–45% higher energy yield annual traditional systems [12]. However, such AI integrated PV framework focus predominantly on silicon or perovskite technologies. Also, these studies highlights the potential of incorporating AI-based forecasting simulations, real-time observation and flexible control to reduce intermittency and environmental restrictions, thereby enhancing definitive and performance of photovoltaic module installations[13].

The present study proposes the fabrication of AI-enabled, organic waste based solar panel comprising luminescent particles extracted from pomegranate and mango peel waste. This polymeric composition matrix increase photovoltaic absorption, particularly in diffuse or low-irradiance environmental conditions. The material innovation is enhanced by an AI analytical network framework that examines irradiance, temperature, electrical output as ultimate panel health monitoring in real time control while enabling predictive ML based diagnostics, efficiency forecasting, and data optimization as described in Fig.1 [14].

Altogether, the bio-optical augmentation and AI-driven control address the functionality management and technological gaps in conventional PV systems, including high environmental footprint. The solution addresses towards waste valorization, reduction in toxic material optimization and management as well as advances bio-solar research focusing on more sustainable and decentralized energy alternatives.

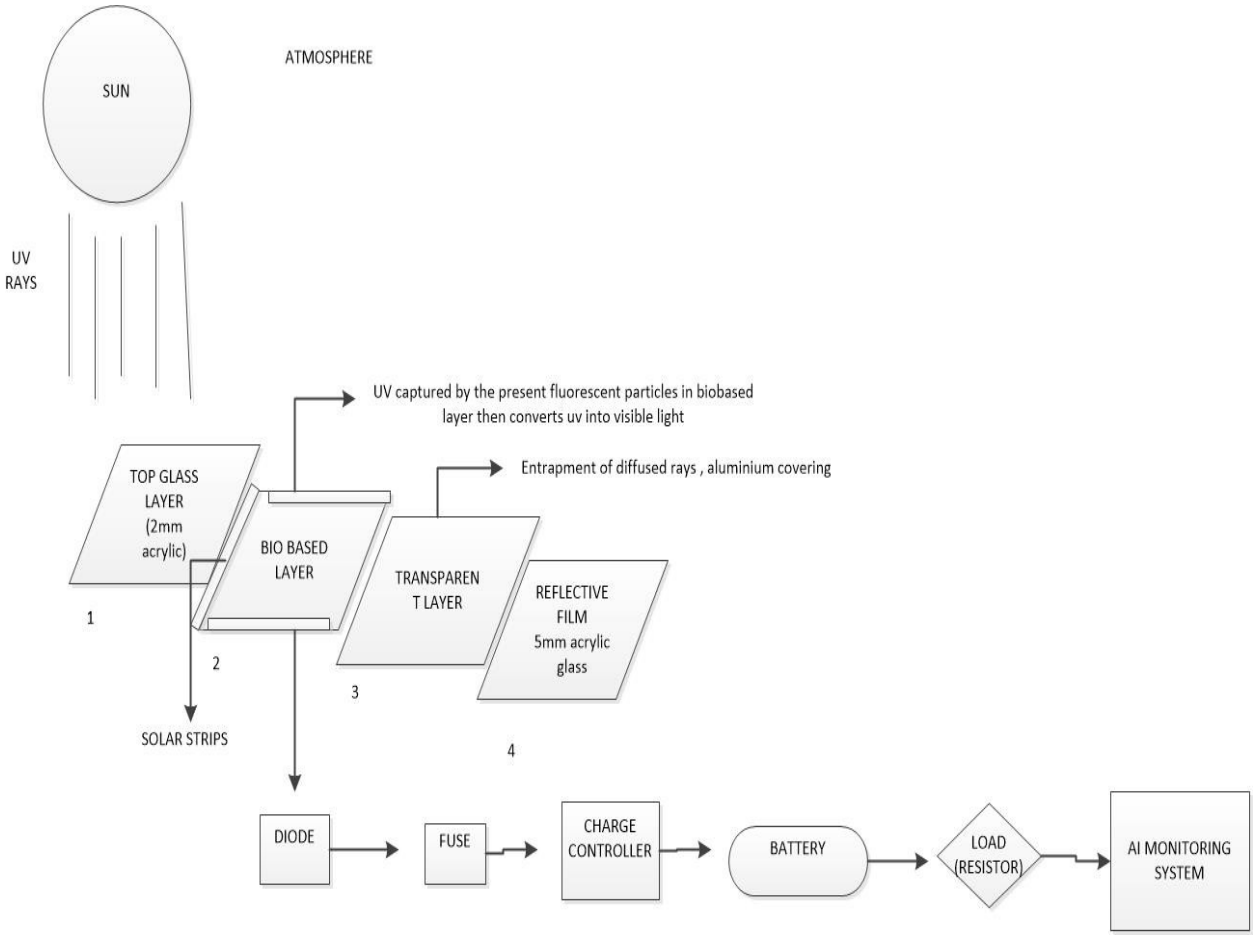


Fig. 1 Technical framework of IoT-AI bio based panel connection

1.2 LITERATURE REVIEW

1.2.1 Limitations of Conventional PV modules

Conventional silicon PV modules express strong reliance on direct irradiance and eliminate 20–40% output under cloudy or less light conditions [15]. Indian studies report large monsoon-related production where temperatures above 45 °C farther reduce efficiency via thermal degradation. End-of panel life raise concerns include non-biodegradable layers, including heavy-metal and limited recycling capacity. Lifecycle analyses exhibit higher carbon emissions during silicon wafer fabrication. These issues highlights an urgent requirement for reduced-carbon, diffuse-light–enhanced PV modules [16]

`1.2.3 Study of Luminescent associated Solar Concentrators (LSCs)

LSCs shows that they improve PV output under different diffuse light by optimizing luminescent materials that ultimately absorb and re-emit photons towards the attached solar cells [17]. Quantum dots, perovskites, and phosphors remain extendedly studied, but also has limitations such as photo bleaching, present toxicity, and non-degradable polymer environmental concerns. Also, high cost and system instability under irradiation restrict the deployment process. Despite having thus the need for ecofriendly solutions [18] .

1.2.4 Phytochemicals extracted as Natural Luminescent Particles

Phytochemicals present in plants and its products like anthocyanin, flavonoids, and carotenoids demonstrate fluorescence and wavelength-shifting properties reliable with PV absorption spectrum. Their presence in fruit waste makes them reduced cost, biodegradable options for optical enhancement films [19] . Prior studies depicts moderate absorption when incorporated into the designed polymer matrices, although the stability persist a challenge [20].

2.4 Sustainable and Bio derived Solar materials

Biodegradable polymers known such as cellulose, cellulose acetate, starch and PLA are progressively explored as an alternate for petroleum-derived encapsulates [21]. These materials decrease carbon footprint and allow safer disposal of modules as compared to conventional waste, providing a solution to limited recycling management. Incorporating agro-waste into the solar components fits well with circular-economy drives and decrease environmental impact [22]. However, very less studies research on bio-based materials which provide optical/luminescent enhancement.

2.5 Artificial Intelligence for Solar Optimization

AI and ML models including LSTM, CNN, Random Forest, and deep-learning architectures remarkably enhance PV forecasting fidelity, fault detection, and real-time monitoring.[23] AI-enabled systems anticipate well irradiance variations, panel degradation, and helps improve overall energy output. Studies since 2020 demonstrate considerable gains in reliability and functional efficiency through intelligent monitoring and predictive patterns [24] .

1.2 OBJECTIVE OF THE THESIS

- To extract luminescent particles from the organic materials such as mango and pomegranate peels utilizing eco-friendly and sustainable approach.
- To examine the optical, luminescent and energy conversion features of the extracted bio-luminescent particles for photovoltaic systems.
- To evolve a bio-inspired luminescent material or covering that can increase the solar panel light absorption capacity and improve energy generation productivity.
- To execute artificial intelligence techniques for solar energy prediction, anomaly detection, and solar panel image classification.
- To advance a sustainable technology by utilizing waste for energy, smart solar monitoring and environment friendly energy results.

CHAPTER 3

METHODOLOGY

3.1 Collection and Preparation of Fruit Peels

Fresh mango and pomegranate peels were collected from the fruit juice shop. The peels were cleaned with thoroughly washing thereby removing all the present dirt and dust particles. The peels were then kept at room temperature only for normal drying around for1 day and then oven dried for about 4 hours at 40 degree Celsius and then finally grinded into fine powder and stored in airtight and clean containers[25].

3.2 Extraction of Luminescent Phytochemicals

For both the fruit peels, 20 g of powder was mixed with ethanol/methanol and were stirred instantly and neck was sealed with aluminum foil and kept on magnetic stirrer for around 2 hours to enhance metabolite extraction. Then the mixture was sonicated for 60 minutes and then rested for 30 min and a clear pink color separate supernatant was observed and a presence of fruity smell indicating correct extraction[26]. The again the process was repeated for stirring the particle and then it was steamed in water bath for 1 hours at 45 degree Celsius. Finally, the filtrate was separated out using thin quality of filter paper. The resulting extract solution was collected using slight evaporation and then stored in amber bottles to prevent from photo degradation.

3.3 Preparation of Luminescent Coating

A transparent acrylic glass plate (15 cm × 15 cm) was cleaned with ethanol. The concentrated extract solution was mixed with 5gm epoxy and hardener base and was uniformly spread over the glass surface and allowed to dry for 12–24 hours resulting in formation of a thin luminescent layer.

3.4 Panel Assembly

The luminescent-coated acrylic glass plate was placed above a silicon strip for consistent optical transmission. The setup was adjusted using tape at the edges to ignore out interference with light.

3.5 Performance Testing

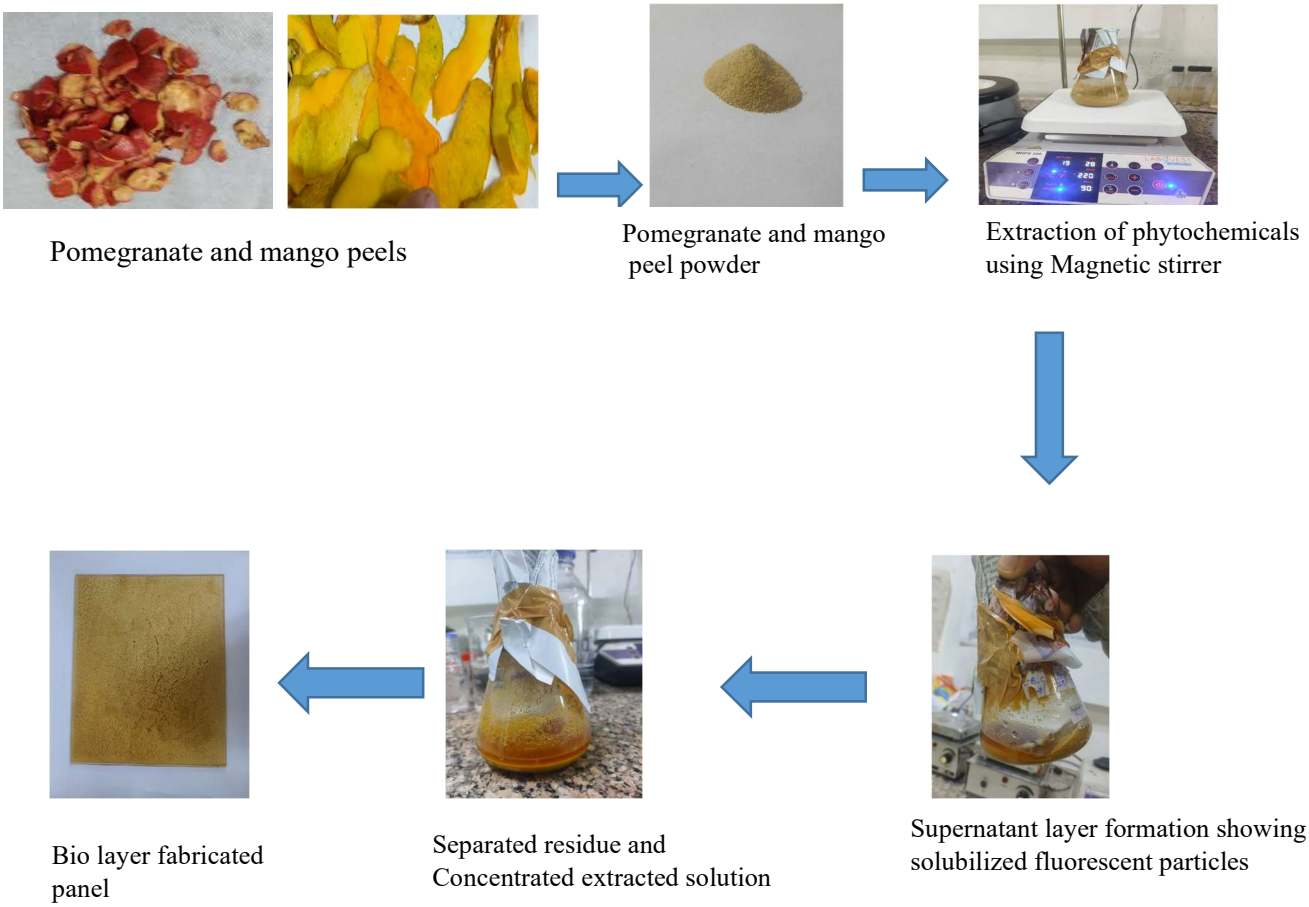
Electrical output readings were recorded using a multi meter having two testing conditions used:

- Direct sunlight (11 AM – 2 PM)
- Diffuse light (cloudy conditions or night light)

For each condition, voltage (V) and current (mA) were recorded and compared with normal solar panel.

Fig. 2 mentioned below explains the detail process of obtaining luminescent particles and panel fabrication.

Fig. 2 : Experimental procedure for procuring luminescent extract solution



CHAPTER 4

Result and Discussion

4.1 Energy Performance Evaluation of Panel

The comparative investigation between the conventional solar panel and the bio-based panel demonstrates a clear improvement in voltage generation over both illumination circumstances. As shown in the Fig.3, the bio based solar panel produced 11.5% increase under direct sunlight compared to the standard module, proving enhanced absorption and re-emission of photons by the submerged fluorescent layer on glass sheet. The second comparison under UV exposure, in which the bio-panel generated 72.2% increase in output as compared to the conventional panel. This substantial improvements indicates successful spectral conversion, permitting the bio-derived luminescent layer to employ high-energy UV photons much more effectively. Overall, the results indicate the functional contribution of the obtained phytochemical layer in improvising light-harvesting efficiency, extremely under conditions were scattered or highly energetic radiation dominates.

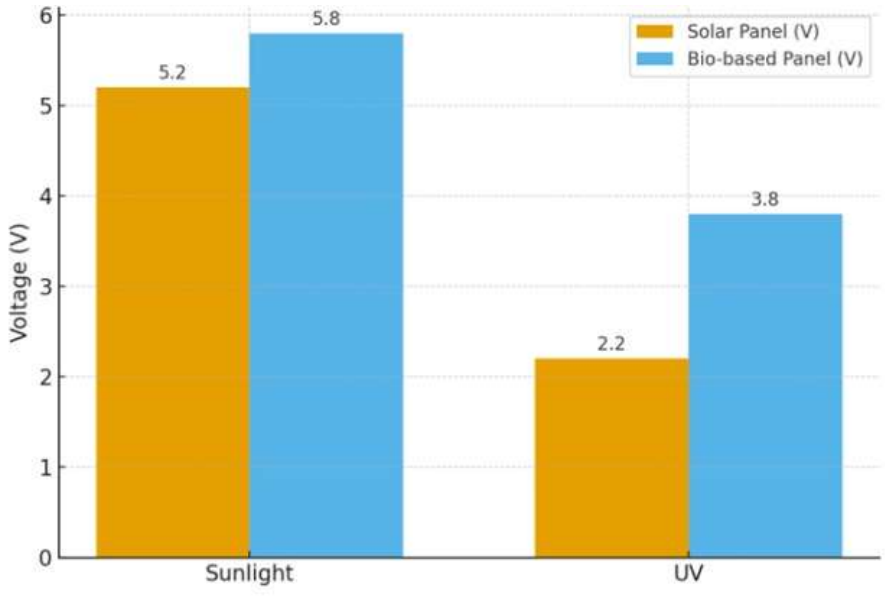


Fig.3 Analysis of energy performance assessment in sunlight and UV

4.2 Analysis of Thermal stability of Panel

Voltage (V) is a definitive indicator of temperature dependent performance in photovoltaic systems as due to open-circuit connection voltage decreases linearly with increase in temperature. This makes comparative analysis of V–T a valid approach for observing thermal degradation as observed in Fig.4. In the present study, the used conventional silicon PV module showed a sharper decrease in voltage with increment in the temperature, compatible with mechanism that cause heat reduction in the semiconductor band gap and thus accelerates electron–hole together recombination, thereby decreasing the panel efficiency. In contrast, the bio-based panel presented comparatively low thermal sensitivity. The bio-luminescent film absorbs higher energy present photons and re-emits at low wavelengths, lowering the direct thermal depression on the silicon films. This reduces the heat-induced efficiency losses and stabilizes the electrical output. The much improved voltage maintenance observed at 35°C and 45°C represents enhanced resistance with concerned to thermal degradation process, highlighting a functional advantage of bio based solar panel.

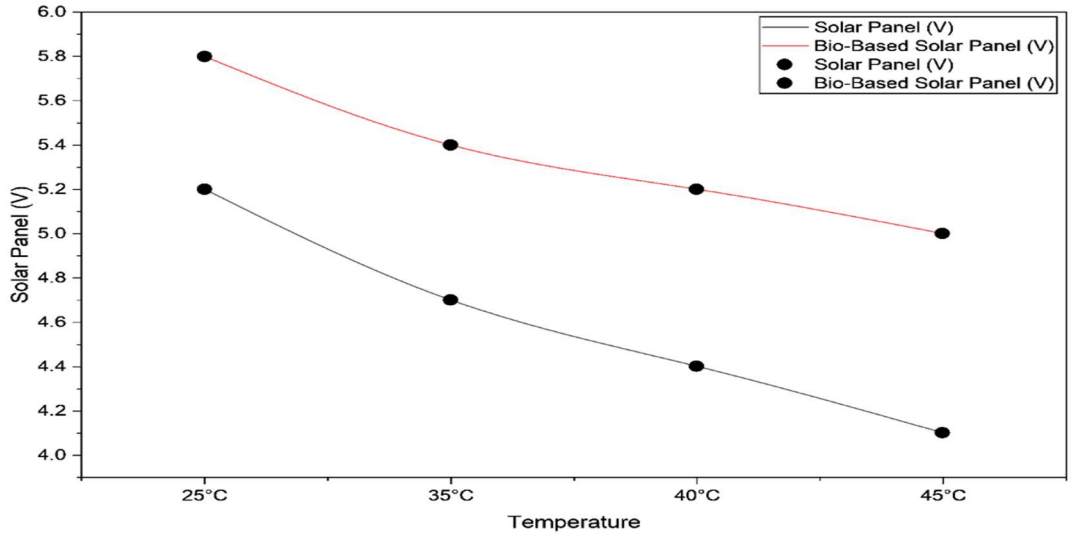


Fig.4 Voltage- Temperature analysis for thermal stability analysis

4.3 Optical Assessment of Bio-Extracted particles

The UV–Visible spectrum of the obtained luminescent solution represent the eminent absorbance peaks at 320nm, 420nm, 540nm and 740 nm as shown in Fig.5 as it directly correlates with the natural optical activity of chromophores present in the extracted solution thereby confirming appropriate extraction of luminescent particles. The peak at observed at 320 nm corresponds well to the UV-A radiation present in atmosphere, which is the main ultraviolet absorbing component indicating that bio-derived particles can well effectively absorb UV-A photons that are general high energy. The other observed peaks at 420 nm, 540 nm, and 740 nm depicting blue, green and near-infrared spectrum region demonstrate broad- light-harvesting pattern behavior. Significantly, all the noticed wavelengths are abundantly present in the natural sunlight, hence, validate the favorable extracted compounds for a real time solar exposure of module. Thus, the uv-vis absorbance profile validates that the luminescent extraction process successfully possess strong optical performance suitable for increasing photovoltaic conduction under open-environment.

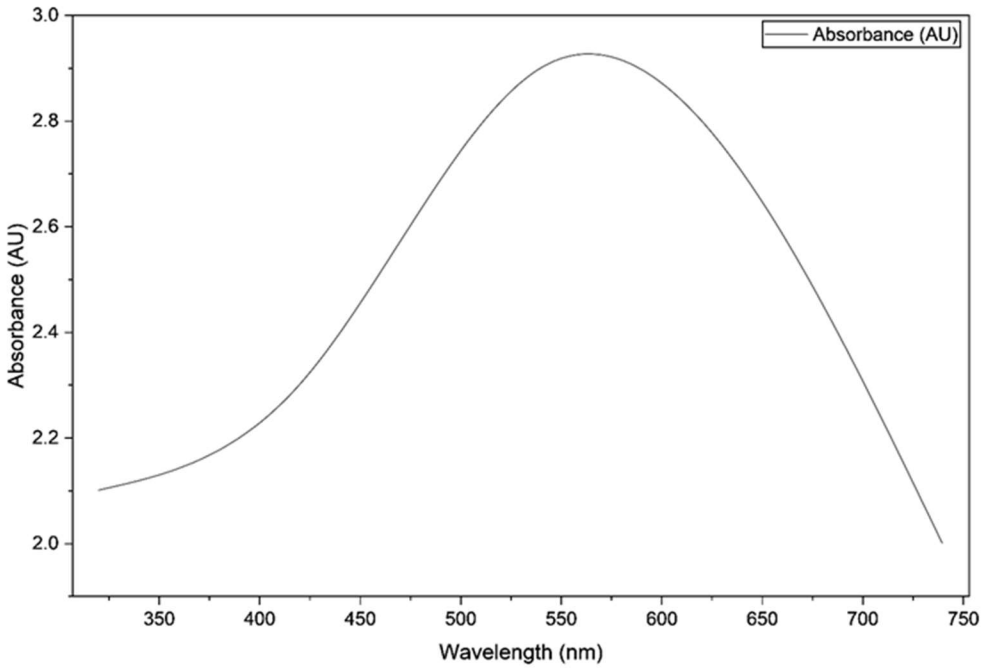


Fig.5 Representation of Luminescent absorbance of UV at different wavelengths

4.4 FTIR

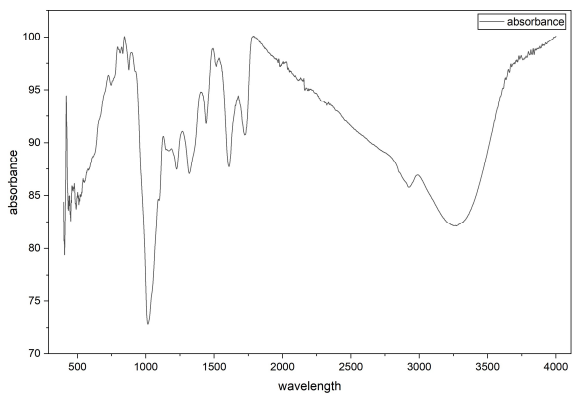


Fig. 6 FTIR analysis of mango and pomegranate Powder

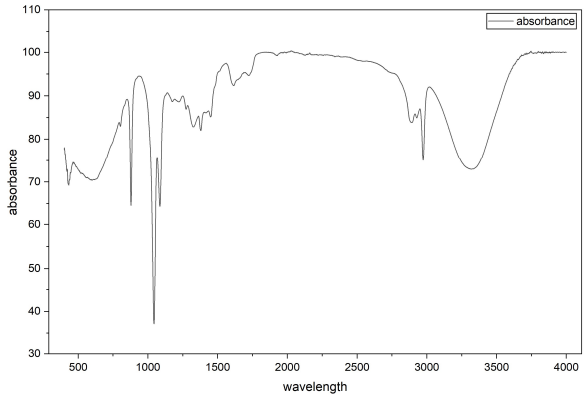


Fig.7 FTIR analysis of luminescent solution

The FTIR obtained of the mango and pomegranate peel powder as shown in Fig 6 exhibits a complex characteristic of plant bio materials particularly rich in polyphenols, carbohydrates as well as organic acids as natural components[27]. A wider absorption band around 3300–3400 cm^{-1} referring to O–H stretching vibrations corresponding to phenolic groups, flavonoids, and the structural polysaccharides[28] . Peaks present in the region 2900–2950 cm^{-1} confirms the C–H stretching of present aliphatic biomolecules[29] . Strong absorptions noticed between 1500–1700 cm^{-1}, majorly near 1600–1650 cm^{-1}, corresponds to C=C stretching due to aromatic rings and amide-related components associated with tannins as well as protein residues[28] . The fingerprint peak region around 900–1500 cm^{-1} shows various peaks linked mainly to C–O, C–O–C, and C–H bending models composed of cellulose, hemicellulose, and bounded polyphenols[30].

After extraction process, the FTIR spectrum obtained of the luminescent solution as mention in Fig 7 exhibit selective enrichment of associated functional groups linked with anthocyanin and flavonoids. The O–H stretching remains near 3300 cm^{-1}, but with due to increased sharpness, it highlights a higher concentration of available phenolic groups[31] . The aromatic C=C stretching region around 1600–1650 cm^{-1} presents as more defined, confirming appropriate solubilization of chromophore structures that corresponds for fluorescence[32].

Also, a huge reduction of polysaccharide-associated in 1000–1200 cm^{-1} peak range suggests successful removal of carbohydrate residues during extraction [33] . Moreover, the region noticed between 2800–3000 cm^{-1} appears comparatively depressed, indicating lower lipid and aliphatic compounds [34].

Therefore, the spectral shifts exhibit the transition from heterogeneous complex composition to a phenolic-rich, chromophore dependent extract [35]. The enhanced groups related to aromatic and hydroxyl-related spectrum absorptions in the luminescent particle solution validate the proper extraction of luminescent compounds majorly anthocyanin, carotenoids and flavonoids mainly responsible for re-emission activity used in bio-luminescent solar panel.

4.5 ENERGY PREDICTION MODEL

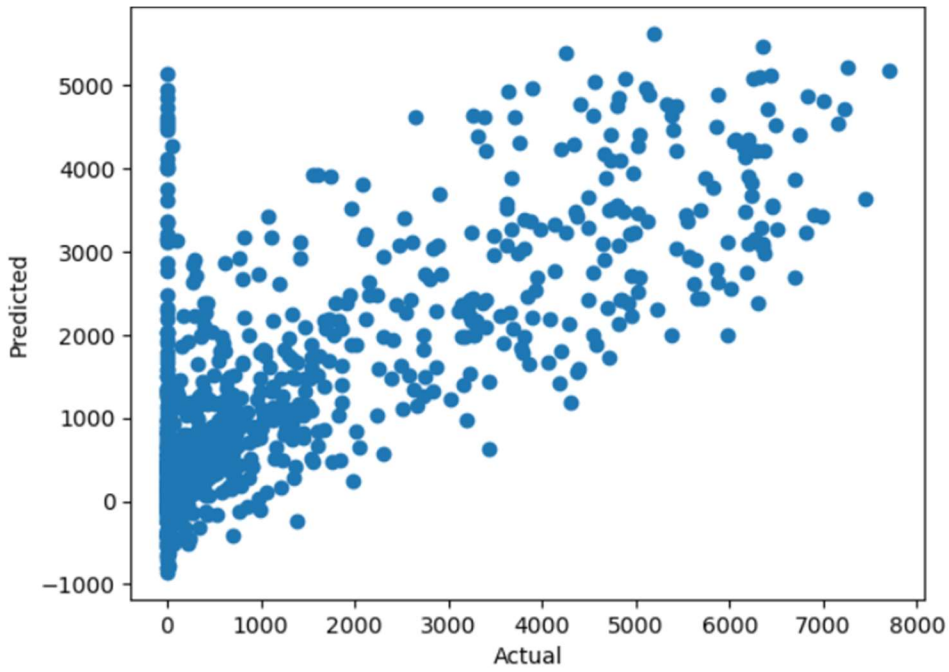


Fig. 8 Graph Interpretation of Energy Prediction Model

The Energy prediction graph plot represented in Fig.8 highlighted the affiliation between the real time energy result and artificial intelligence based energy output obtained using the most appropriate Random Forest Regression model. The graph in the x-axis presents the actual energy values associated from the photovoltaic datasets, whereas the y-axis presents the communicated predicted energy data generated by the respective machine learning model. Every individual point shown on the scatter plot relates to the one testing monitoring from the available dataset used during model examination.

In a real time prediction system, all the available data points would lie exactly along a straight diagonal line, highlighting the predicted energy values are truly equal to the actual measured outcomes. Therefore, in practically applicable energy forecasting operations, perfect spatial positioning is rarely obtained because solar energy generation is highly dependent on variable environmental as well as aerial conditions. Affecting factors defined as fluctuating solar radiation, variable cloud movement, differentiable wind speed, noticeable change in humidity, atmospheric

air and pressure significantly authority photovoltaic energy generation and initiate the uncertainty into the foreseen activity.

The graph illustrate a true positive relation in between the actual and predicted energy outcome. With due course, the actual energy production inflates, the expected values also incline towards increase shift, thereby confirming that the Random Forest Regression model successfully mastered significant relationship between affecting environmental parameters as well as system production manner. This positive pattern confirms that the associated machine learning model adapted value driven hidden sequence pattern from the dataset in replacement of generating arbitrary predictions.

An observational clustering and dispersion of points can be notices near decreased actual energy values, especially around zero as well as low-production locations. This variation express that prediction accuracy lowers during unstable environmental requirements where solar generation fastly varies invariably. Such behavior is oftenly observed in solar voltaic forecasting organized framework systems due to sudden differentiation in irradiance, shading consequence, weather balance, and sensor noise associated in the real-world photovoltaic datasets.

Additionally, some prediction points are distributed away from the initial trend region, presenting the proximity of prediction errors and moderate forecasting restrictions. Nevertheless, the overall ascending pattern of the scatter plot ensures that the generated AI-based Random Forest model is extremely capable of executing trend-defined energy prediction with accomplished performance. Therefore, the graphical estimations confirms the application based feasibility of integrating machine learning models into intelligent and smart solar energy examination and prediction for energy systems.

4.5.1 Environmental Parameters - Solar Energy Prediction

	Date-Hour(NMT)	WindSpeed	Sunshine	AirPressure	Radiation	AirTemperature	RelativeAirHumidity	SystemProduction
0	01.01.2017-11:00	1.1	46	1005.8	49.7	-0.2	74	215.8333
1	01.01.2017-12:00	1.2	60	1006.1	138.7	1.8	72	831.6667
2	01.01.2017-13:00	0.4	59	1006.1	121.6	2.7	66	349.5000
3	01.01.2017-14:00	4.0	55	1006.5	77.0	5.0	49	272.0000
4	01.01.2017-15:00	2.7	26	1007.6	33.1	4.8	48	130.2083

Table.1 Dataset - environmental and meteorological parameters

The above dataset in Table.1 represents the environmental as well as meteorological parameters used for integrating the solar energy prediction framework. These parameters were composed to analyze the characteristics of atmospheric conditions on photovoltaic operation performance and energy production. Each character depicts an important position in determining the optimization and power results of the solar panel system.

The Date-Hour (NMT) parameter represents the time value of each noticeable recorded in Nepal Mean Time (NMT). This parameter assist in understanding the temporal difference of solar energy generation all through time zones and days. Solar production is majorly conditional on time due to the fact that sunlight intensity varies continuously during the day.

Wind Speed represents the travelling speed of wind in the surrounding atmosphere. Wind speed affects the cooling of associated panels. Greater wind speed can decrease panel temperature, thereby working upon photovoltaic efficiency and energy production under certain environment.

Sunshine presents the duration of sunlight received by the solar panel plates. It is one of the most significant parameters because photovoltaic systems directly impact on sunlight presence for electricity production. Higher sunshine duration commonly outcomes as in higher energy production.

Air Pressure represents atmospheric air pressure in the environment. Changes in the atmospheric pressure are often related with weather conditions such as cloudy, storms, or clear skies, which indirectly results in solar irradiance and system performance.

Radiation indicates to the solar radiation or irradiance approaching the solar panel surface. This parameter has explicit relationship with energy generation because greater radiation levels enhance photon absorption and electricity output in photovoltaic cells.

Air Temperature represents the surrounding atmospheric temperature. Although sunlight multiply energy production, exceeding high temperatures can decrease photovoltaic efficiency as the solar cells bears thermal losses at shifted temperatures.

Relative Air Humidity measures the moisture amounts present in the surroundings. High humidity can decrease solar irradiance arriving the panel surface because to scattering and assimilation effects in the surrounding, thereby implementing energy output.

Finally, System Production highlights the actual electrical energy production by the photovoltaic system. This is the objective variable optimized for training and examining the machine learning prediction model. Thereby, analyzing relationships in between the environmental parameters as well as system production, the AI-defined Random Forest Regression model trained to forecast solar energy generation patterns productively. Overall, the dataset supports all inclusive environmental information important for intelligent solar energy prediction and maintaining energy monitoring.

4.5.2 ENERGY PREDICTION – CONFUSION MATRIX

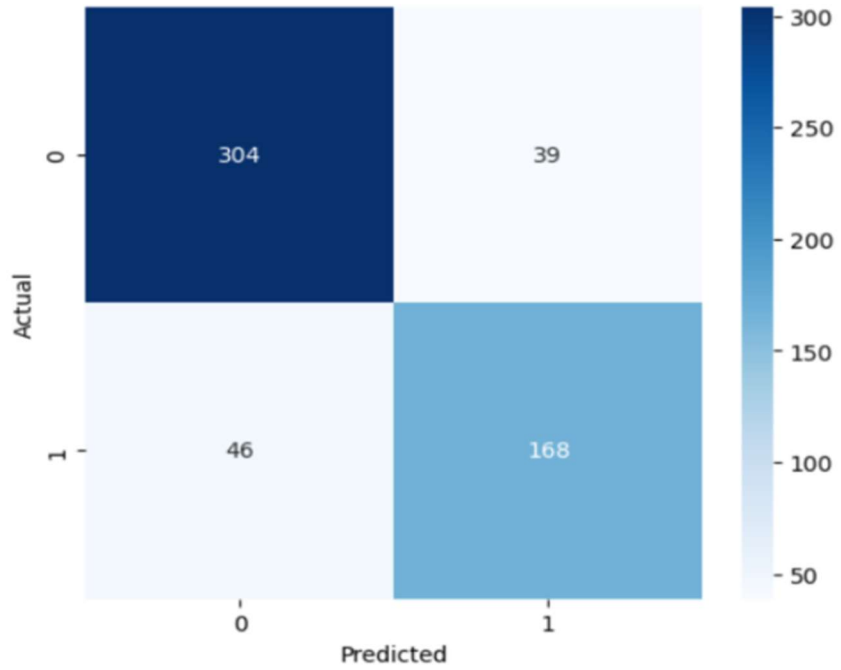


Fig. 9 Confusion Matrix of Energy Prediction

The above Fig. 9 confusion matrix highlights the performance of the Energy Prediction model by related actual values with predicted data. In this matrix, the rows suggests the actual classes, while the columns represent expected classes. The data values within the matrix represents the count of correctly and incorrectly classified samples. The matrix mainly comprised of four important parts namely: True Positive (TP), True Negative (TN), False Positive (FP), and False Negative (FN).

The value present at 304 at the top-left corner suggests for the True Negative (TN) count. This signifies that this samples actually associated to class 0 and were also rightly predicted as class 0 by the approach of this model. This represents strong performance in recognizing normal or non-fault energy environments.

The value present in 168 at the bottom-right corner suggest the True Positive (TP) count. These samples that actually associate to the class 1 and were rightly predicted as class 1.

This signifies that the model was capable to successfully detect an important number of positive or high-energy situations.

The value present in 39 at the top-right corner suggest the False Positive (FP) count. These samples actually associate to class 0, whereas the model analyzed them as class 1 incorrectly. Also, the present False positives represent as incorrect alarms or redundant positive predictions made by the approach of this model.

Similarly, the value present in 46 in the bottom-left corner suggest the False Negative (FN) count. These samples actually associate to class 1, but the model incorrectly analyzed them as class 0. False negatives are significant because the model failed to recognize actual positive energy situations.

The confusion matrix thereby presents that the model outcomes as good predictive performance associated with high True Positive and True Negative values. However, the indication of False Positives and False Negatives signifies that some prediction errors still remains. Working upon these errors by following hyper parameter tuning approach, featuring engineering, or advanced machine learning methods can further correct upon the accuracy and reliability of the energy prediction system.

4.6 ANOMALY DETECTION MODEL

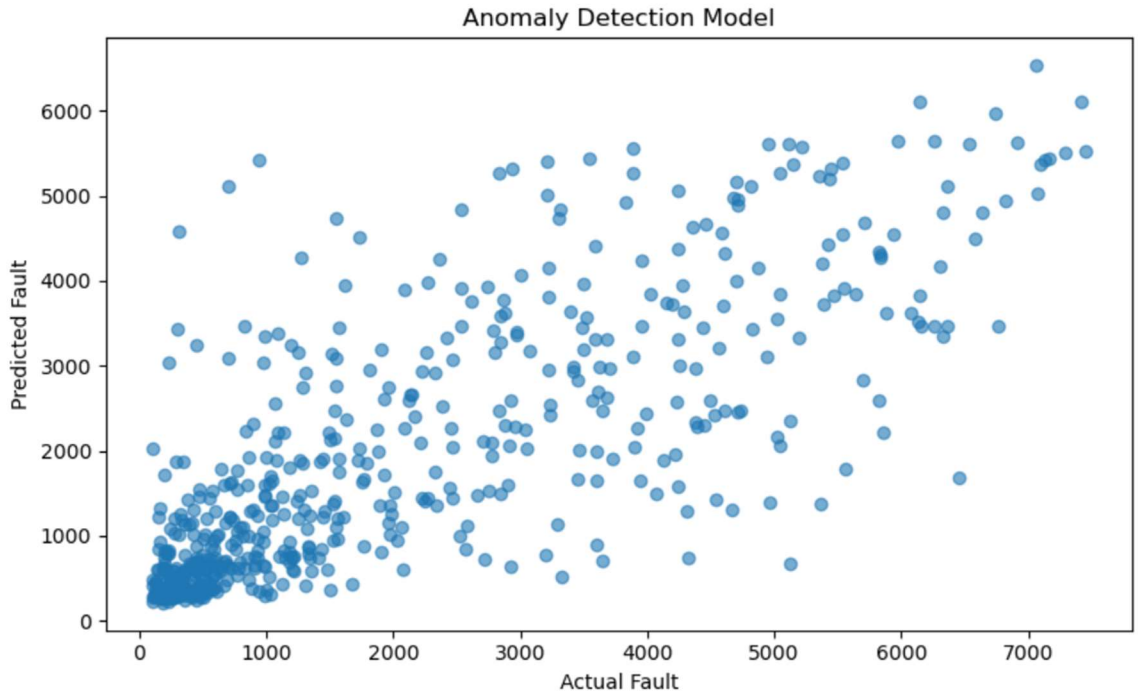


Fig. 10 Anomaly Detection Model for panel system

The above Fig.10 scatter plot represents the Artificial intelligence based anomaly detection model for performance analysis of intelligent bio-fluorescent solar panel. The graph co relates with the actual fault related values estimated from the known dataset with the predicted value data obtained by the most suitable machine learning model. The x-axis herein represents the actual observed system pattern, whereas the y-axis represents the value set data predicted by the respective model during testing phase.

The graph represents a generally increment in trend, signifying that the model has successfully learned the co-relationship between environmental and energy parameters related with anomalous or faulty working conditions. With the due course, actual values elevate the predicted values also

thereby patterned to increase, presenting that the Random Forest-based Artificial intelligence model can accomplish patterns desired towards system discrepancies and operational elevations.

An important concentration of data points is admirable in the lower-left section of the graph. This indicates that major operational conditions in the known dataset results towards lower or normal anomaly sections. Such defined clustering is commonly often in real time monitoring systems because error in associated events commonly occur less repeatedly than normal operating situations. The model performs likely well in this decreased operational range, which is significant for constant real-world monitoring applications.

At higher values, the values of data point results wider, signifying some prediction variability for more sophisticated or severe anomalous data points. This variation outcomes varies from nonlinear environmental functions, IoT sensor noise, variable irradiance, or unstable electrical behavior in the solar prototype framework. Despite this invariance, the overall positive pattern confirms that the Artificial intelligence model can greatly receive fault-related behavioral trend.

The graph authenticate the feasibility of incorporating artificial intelligence into smaller level solar monitoring architecture for anomaly verification and predictive diagnostics. Therefore, for an experimental prototype functioning under true environmental conditions and restricted training data, the generated prediction behavior is highly scientifically acceptable. This graphical evaluation approach are widely optimized in renewable energy forecasting as well as intelligent fault detection investigation to assess the practical execution of machine learning models

4.6.1 ANOMALY DETECTION – CONFUSION MATRIX

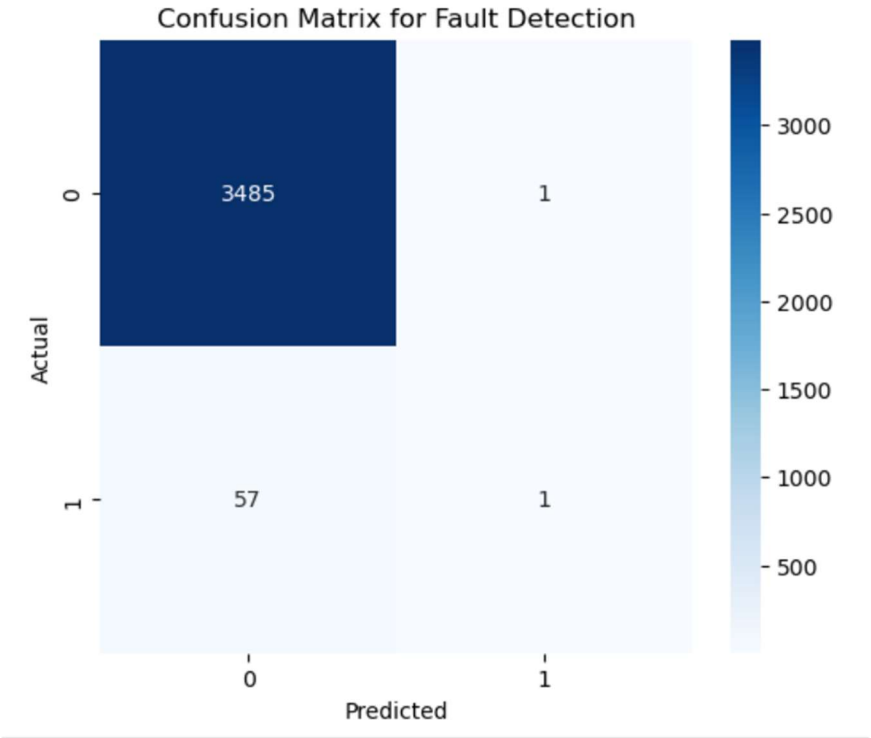


Fig.11 Confusion matrix of Anomaly detection model

The confusion matrix in Fig.11 represents the anomaly or fault detection model depicts the classification performance evaluation of the machine learning algorithm in distinctive between normal and faulty functioning conditions of the associated solar panel system. In the above matrix, class “0” showcase the normal condition, whereas the class “1” presents the anomaly or fault condition.

The upper-left data value (3485) presents the True Negatives (TN), shows that 3485 normal instances were appropriately classified as normal by the respective model. This high result value demonstrate that the system performs considerably well in recognizing healthy operating

conditions without obtaining unnecessary fault alarms. The upper-right data value (1) presents the False Positives (FP), wherein one normal circumstance was incorrectly identified as faulty.

Such a low false alarm level is highly noticeable in practical photovoltaic monitoring systems as they offer excessive false alerts causing reduction in operational reliability and shift in maintenance costs as well.

The lower-left data value (57) presents towards the False Negatives (FN)**,** which depicts that 57 faulty cases were wrongly classified as a normal case. This highlights that some anomalies were not yet detected by the defined model. In the solar energy systems, false negatives are significant because undetected faults results in reduction of energy efficiency as well as long-term system performance. Also, the lower-right data value (1) presents the True Positives (TP), showcasing that only one anomaly was rightly identified as an error fault.

The matrix depicted that the dataset is mainly imbalanced, often with a significantly larger count of the normal samples relative to the anomaly samples. Such imbalance often occurs in real-world fault detection systems as these faults are commonly rare circumstances. Due to this irregular situations, the model highlights more biased predicting to the majority class (normal condition), which highlights the lower anomaly detection ability performance.

Along with this limitation, the model successfully illustrate the feasibility of Artificial intelligence based anomaly detection system in photovoltaic operations. The results highlights that the algorithm can mainly effect the learn operational patterns and recognize deviations from normal behavior. Although, further refinements may be achieved utilizing balanced datasets, as well as synthetic anomaly production, oversampling techniques, or higher deep learning framework to enhance fault recognition results.

4.6.1 EVALUATION METRIC OF ANOMALY DETECTION PERFORMANCE

S. No.	Evaluation Metric	Obtained Value	Description
1	Accuracy	98.0%	Overall anomaly detection performance
2	True Positives (TP)	1	Correctly detected anomaly samples
3	True Negatives (TN)	3485	Correctly identified as normal samples
4	False Positives (FP)	1	Normal samples incorrectly classified
5	False Negatives (FN)	57	Missed anomaly detections
6	Precision	50.0%	Correct anomaly predictions among detected anomalies
7	Recall (Sensitivity)	1.72%	Ability to detect actual anomalies
8	F1-Score	3.33%	Harmonic balance between precision and recall
9	Specificity	99.97%	Correct identification of normal conditions
10	False Positive Rate (FPR)	0.03%	Rate of false anomaly alarms
11	False Negative Rate (FNR)	98.28%	Rate of missed anomalies
12	ROC-AUC Score	0.51 (Approx.)	Model discrimination capability
13	Model Type	Anomaly Detection Model	Binary fault detection system
14	Prediction Target	Fault Detection	Identification of abnormal operational behavior
15	Input Variables	Sensor/System Features	Features used for anomaly prediction

Table.2 Anomaly detection performance evaluation

The performance evaluation table represented in Table.2 of the defined anomaly detection model results in the effectiveness and restrictions of the system in recognizing abnormal operational conditions. The model accomplished an overall accuracy of 98%, highlighting that the majority of samples were classified correctly. Also, the confusion matrix, model accomplished completely identifying 3485 normal samples as normal (True Negatives) and often correctly detected 1 anomaly sample (True Positive). Although, 57 anomaly outcomes were incorrectly classified as normal (False Negatives), whereas only 1 normal sample was no classified as anomalous (False Positive).

Also, the overall accuracy resulted as very high and further analysis shows that the dataset is highly imbalanced, occurring with significantly more normal samples in comparison with anomaly samples. Due to this defined imbalance, accuracy alone enough does not provide a secure measure of model performance. The associated precision value of 50% highlights that half of the detected anomalies were rightly identified. Although, the recall value of 1.72% is very low, showing that the model failed to identify the most anomaly cases. Accordingly, the F1-score presenting 3.33% also restricts low, reflecting towards poor balance in between the precision as well as recall.

The specificity defined as 99.97% indicates excellent performance in recognizing normal operational situations. Also, the very low False Positive Rate (0.03%) presents that the model rarely produced the false alarms. Since then, the False Negative Rate 98.28% highlights that most anomalies were unidentified, which limits the efficiency of the system for real-world fault detection functioning.

Overall, the model functions performs effectively for normal condition recognizing but requires further optimizing in anomaly detection competence. Future increments in results may include data balancing methods, oversampling approach, threshold optimization, and highly advanced deep learning technique to improve recall as well as anomaly detection performance.

4.7 IMAGE CLASSIFICATION MODEL – CNN

[3]:

	irradiance	temperature	voltage	current	power	fault
0	24.835708	26.561841	22.302774	0.579492	12.924288	0.0
1	79.045464	25.589033	23.504519	0.418080	9.826768	0.0
2	38.470697	25.200372	23.573217	0.285432	6.728549	0.0
3	0.000000	25.207802	23.152138	0.131588	3.046549	0.0
4	0.000000	25.388358	20.247466	0.087994	1.781647	0.0

Table.3 Parameters Used for Anomaly Detection Model

The above dataset in Table.3 represents the electrical and environmental parameters used for generating the anomaly detection model for the associated solar photovoltaic system. These parameters were obtained because they directly impact the solar panel performance as well as help in identifying the abnormal working conditions, faults, or efficiency reduction in the defined system. The anomaly detection model thereby analyzes these parameters to differentiate between normal and faulty working conditions of the solar panel.

Irradiance parameter typically highlights the measure of solar radiation transmitting directly as well as indirectly at the surface of the solar panel. It defines as one of the most essential parameters because solar energy generation is mainlyS associated directly on sunlight intensity. Amount is as much higher irradiance generally results in an increased current production and improved power output, whereas sudden drops in irradiance may demonstrate cloudy conditions, shading, or environmental distraction.

The temperature parameter signifies the operating temperature of the solar panel and surrounding environment. Temperature majorly affects photovoltaic efficiency results. Moderate temperatures support confined operation, in place of excessive heating can decrease panel efficiency, increase in resistance, and decreased voltage result. Therefore, monitoring temperature is an important factor for recognizing thermal anomalies and abnormal working conditions.

The voltage parameter presents the electrical overall potential generated by the photovoltaic system. In between Voltage fluctuations may depicts problems such as panel degradation, loose connections, shading effects, or system inaccuracy. Stable voltage therefore generally represents healthy panel operation.

The current parameter counts for the flow of electrical charge produced by the solar panel. Current production is directly impact to the solar irradiance. The low current values under high irradiance conditions may describes the attached faults such as dust accumulation, broken cells, or partial shading conditions.

The power parameter presents the actual electrical power produced by the photovoltaic system. It is oftenly calculated using voltage and current outcomes. Different variations in power output are strongly indicates of a system efficiency and operational functioning. Significant differentiation from predicted power generation may highlight anomalies or performance corrosion.

At the end, the fault parameter presents the target result used in anomaly detection. In the defined dataset, a value of 0 generally signifies normal operating conditions, whereas a value of 1 demonstrate faulty or anomalous conditions. The associated machine learning model uses the intersection of among irradiance, temperature, voltage, current, and power to analyze abnormal behavior automatically.

Overall, these parameters provide explanatory information about the electrical and environmental condition of the solar photovoltaic system and enabled intelligent Artificial intelligence based anomaly detection for properly solar energy monitoring and fault diagnosis.

4.7.1 PERFORMANCE EVALUATION OF CNN MODEL

Parameter	Clean Class	Dusty Class	Snow Class	Overall Performance
Precision	0.51	0.34	0.19	0.40
Recall	0.49	0.34	0.21	0.39
F1-Score	0.50	0.34	0.20	0.40
Support (No. of Samples)	298	213	84	595 Total Samples
Training Accuracy	—	—	—	82.74%
Validation Accuracy	—	—	—	78.32%
Training Loss	—	—	—	0.4074
Validation Loss	—	—	—	0.5036
Number of Epochs	—	—	—	30 Epochs
Batch Size	—	—	—	32
Optimizer Used	—	—	—	Adam Optimizer
Activation Function	ReLU / Softmax	ReLU / Softmax	ReLU / Softmax	CNN Architecture
Image Size	64×64 Pixels	64×64 Pixels	64×64 Pixels	Standardized Input
Number of Classes	Clean	Dusty	Snow	3 Classes
Classification Type	Multi-Class	Multi-Class	Multi-Class	Image Classification
Over fitting Observation	Moderate	Moderate	Moderate	Controlled

Table.4 Performance evaluation of CNN model

9 The above Table.4 represents the detailed performance evaluation of the Convolutional Neural Network (CNN) deployed for obtaining the classification results of solar panel conditions. The model was efficiently trained to classify different solar panel images into mainly three categories: Clean, Dusty, and Snow-covered. Multiple evaluation parameters defined as the precision, recall, F1-score, accuracy, and losses were used to calculate the accuracy of the model.

Precision in model measures mainly the accuracy of the model predicting the particular class. The Clean class obtained the highest precision value of 0.51, reflecting that the model was co-relatively better at recognizing clean solar panels images. Whereas the Dusty and Snow classes' images achieved lower precision outcome values of 0.34 and 0.19 respectively, implicating that the model covered challenges in differentiating dusty and snowy panels because of the associated similarities in texture and lighting conditions.

Recall parameter indicates the capability of the model to rightly detect actual images attaching to each class. The recall outcome values were 0.49 for Clean, 0.34 for Dusty, and 0.21 for Snow. These results depicts that the CNN model was more completely trained in identifying clean panels rather than snow-covered panels. The F1-score collaborates the precision value as well as recall value into a single metric, significantly followed a similar pattern with values as 0.50, 0.34, and 0.20 for Clean, Dusty, and Snow classes respectively.

The model thereby achieved a training accuracy level of 82.74% and validation accuracy level of 78.32% after 30 epochs trail, demonstrating good learning capability and generalization ability. Training and validation losses of 0.4074 and 0.5036 respectively demonstrate that the model effectively decreased the classification errors during the training phase. The CNN architecture used ReLU and Softmax working functions with the Adam optimizer having a batch size of 32.Therefore, Overall the model describes the satisfactory performance for programmed solar panel condition monitoring as well as image-based fault detection as practical applications.

4.7.2 CNN MODEL PERFORMANCE BASED – CONFUSION MATRIX

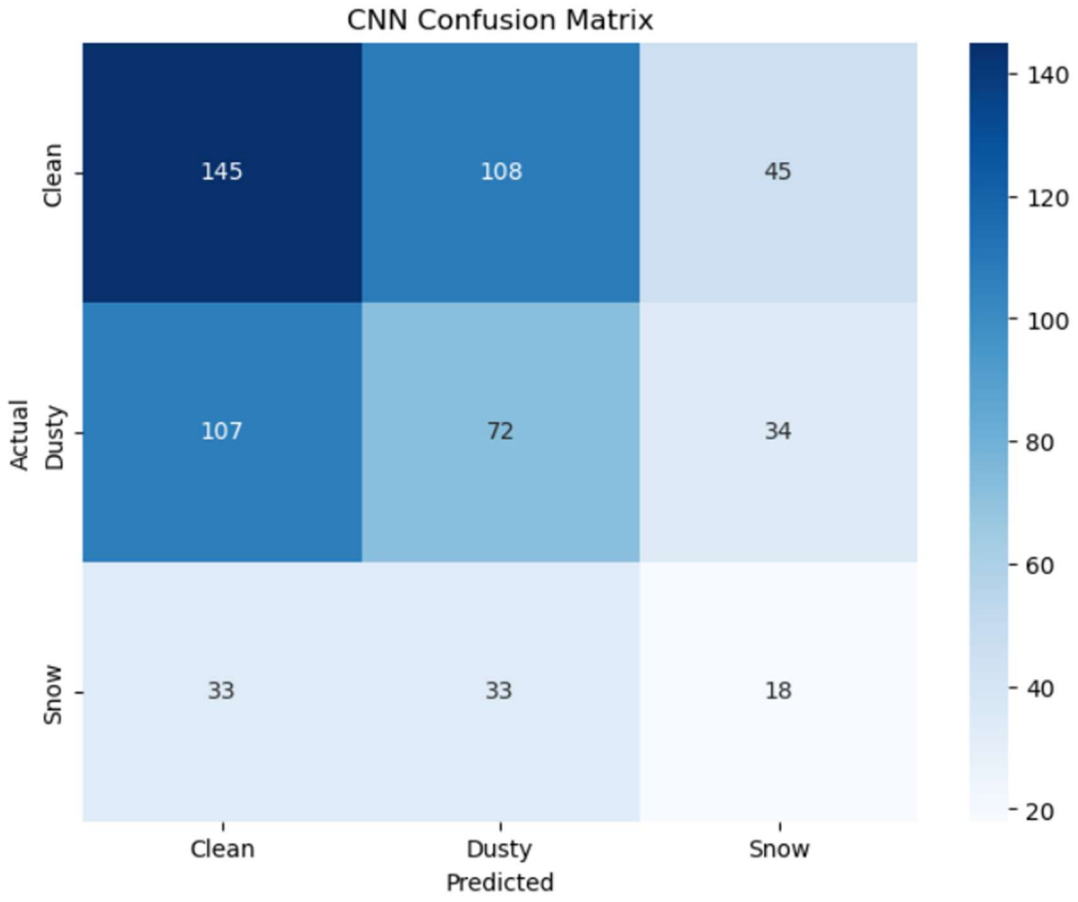


Fig.12 Confusion matrix evaluation of CNN model

The CNN based Confusion Matrix in Fig.12 provides an explanatory evaluation of the classification presentation of the Convolutional Neural Network for mainly three classes: Clean, Dusty, and Snow-covered solar panels. In this matrix above, the rows presents the actual classes, whereas the columns presents predicted class obtained by the CNN model. The diagonal values present correct predictions, represented as True Positives (TP), while the opposite off-diagonal values highlight the incorrect classifications, which comprise of False Positives (FP) and False Negatives (FN). True Negative (TN) values present rightly ignored samples belonging to different classes.

For the Clean class, the CNN model accurately classified 145 images defined as Clean, presenting the True Positive value for the clean category. However, 108 clean images were incorrectly classified as Dusty. Whereas 45 images as Snow, contribute to the False Negative predictions for the defined clean class. Similarly, images from other different categories incorrectly predicted as Clean demonstrate towards the False Positives. This represents that although the model recognized many clean panels correctly, it faced confusion between clean and dusty panels may be due to visual matchings.

For the Dusty class, the CNN model correctly predicted 72 images as Dusty (True Positive). However, 107 Dusty images were incorrectly predicted as Clean. Whereas the 34 as Snow images contributed to the False Negative values. Miscategorization occurred because of the some dusty panels visually related to the clean surfaces under differentiable illumination conditions.

For the Snow class, only defined 18 images were correctly identified and classified as Snow, representing the lowest True Positive value among all the categories. Meanwhile, 33 Snow images were misclassified as the Clean and another 33 as the Dusty, resulting in the higher False Negative values. This lower performance evaluation may be attributed to restricted snow samples and similarities in brightness trends among the different classes.

Therefore, overall the confusion matrix highlights that the CNN model successfully learned significant visual features of the solar panel classification. However, the proximity of False Positives and False Negatives depicts that further enhancements such as dataset balancing, image augmentation, transfer learning, or YOLOv8 implementation could in future enhance classification accuracy and decrease the misclassification errors.

4.7.3 CNN MODEL ACCURACY AND LOSS DEPICTION

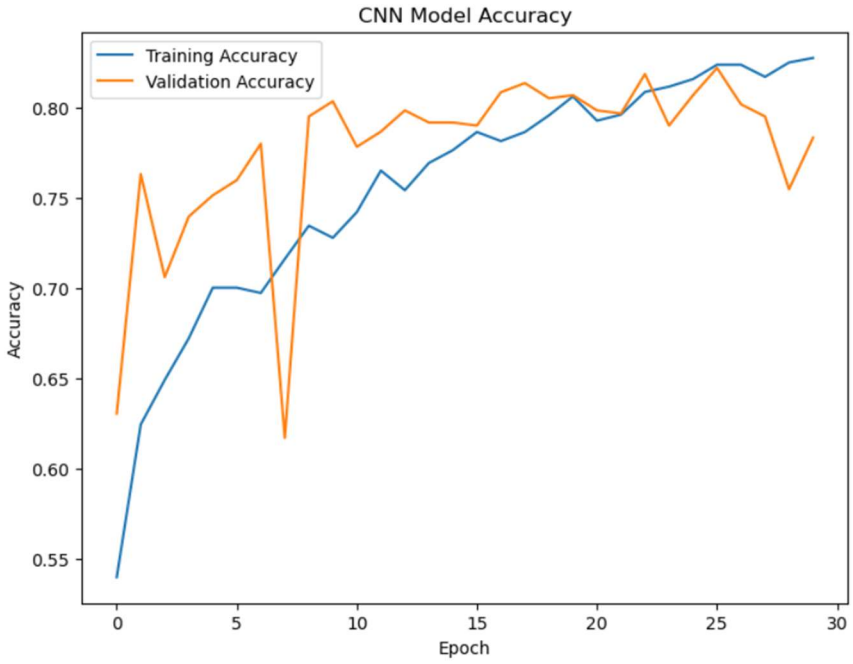


Fig.13 Representation of CNN model based accuracy graph

The CNN Model Accuracy graph in Fig.11 presents the learning performance evaluation of the Convolutional Neural Network during the training and validation phases over 30 epoch's trails. In this graph, the blue line depicts the training phase obtained energy accuracy outcome, whereas the yellow line highlights validation phase associated accuracy. The x-axis typically denotes counts of different epochs whereas the y-axis presents the classification accuracy accomplished by the model.

Initially, the training accuracy initiated at approximately 54%, highlighting that the model had restricted understanding of image trends in the early stages. As the epochs incremented, the training accuracy frequently improved and finally approached nearly 83%, showing that the CNN model successfully learned phase importantly visual features from the solar panel dataset comprising of Clean, Dusty, and Snow-covered panels. The gradual increment in training accuracy highlights effective feature extraction and instructions capability of the CNN framework.

Similarly, the validation accuracy also worked upon the significantly during training phase. It variance across different trend epochs due to variations in validation samples and presented dataset imbalance, but total it maintained a stable upward pattern.

The highest validation accuracy accomplished was approximately 82%, which signifies good generalization capability of the model on unnoticeable images. The proximity relationship between training phase and validation phase accuracy suggests that present model could not suffer from severe overfitting practices.

The graph also demonstrated that after around trying 20 epochs, both curves became relatively confined, indicating that the model had accomplished near-optimal learning performance evaluation. This describes that increasing multiple epochs helped improve feature learning phase and image classification performance model. Overall, the accuracy graph affirms that the CNN model was productive in classifying solar panel conditions and successful satisfactory performance for obtaining computer vision-based solar anomaly fault detection practice.



Fig.13 Representation of CNN model based Loss graph

The CNN Model Loss graph in Fig.12 signifies that the reduction in prediction faults during the training and validation phase, procedure of the Convolutional Neural Network. In the graph, the blue line highlight training loss, although the yellow line depicts validation loss various 30 epochs.

The x-axis demonstrate epochs, whereas the y-axis presents the loss values obtained by the categorical cross-entropy loss working.

At the initial of training phase, the training loss was comparatively high, approximately 0.90, which depicts that the model starting made many incorrect predictions whereas classifying solar panel images. However, as training phase progressed, the training loss continuously reduced and finally reached approximately 0.40. This decrease demonstrates that the CNN model commonly learned meaningful image trends and worked upon its classification capability over time.

The validation loss also highlighted an overall decreasing trend, also some fluctuations were noticed during intermediate epoch's counts. These fluctuations are often in deep learning models and usually happens due to differentiate in validation samples, image invariance, or dataset imbalance. Despite minor changes, the validation loss remained near to the training loss, signifying that the present model commonly impacts on the unnoticed data sets as they did not experience any important over fitting conditions.

The graph further represents that after approximately 15–20 epochs trends, both training and validation losses stabilized particularly. This representation of the CNN model achieved convergence and learned phase optimal features from defined dataset. Lower loss values correlates to the improved prediction capability and improvised classification accuracy.

Hence, overall the loss graph signifies that the CNN model successfully decreased classification errors during training phase. The decrementing loss values, along with the stable validation performance, highlights that the model is reluctant for identifying Clean, Dusty, and Snow-covered solar panel images in solar energy examining systems.

CHAPTER 5

CONCLUSION

This study illustrate the successful development and initial evaluation of a bio luminescent solar layer synthesized from mango and pomegranate peel powder extracts. The characterization of the chromophores majorly anthocyanin, carotenoids and flavonoids using UV–Vis spectroscopy confirmed the strong absorbance across various functionally reliable solar wavelengths around (320–740 nm), while FTIR analysis also verified the enrichment of phenolic and aromatic components responsible for fluorescence-based photon re-emission range [36]. When inter related with conventional silicon PV wafers, the bio-luminescent film exhibited noticeable performance enhancement under the both required condition i.e. direct sunlight and diffuse UV at shady conditions, yielding much higher voltages than the comparable control panel. Further, the temperature–voltage analysis validated reduced thermal sensitivity present in the bio-panel, indicating issues related to the thermal degradation process through photon conversion and moderated heat loading depression on the silicon component.

The use of fruit peel waste demonstrate the technology associated with the sustainable circular-economy concept and addresses main limitations of traditional solar modules globally and India, including higher cost, lower functional efficiency under dark conditions, and environmental issues associated with hazardous panel waste[37]. Overall, the results validate well with the potential of budget friendly cost, biodegradable luminescent particles as performance increasing optical layers for development of next-generation photovoltaic module systems, with reliance to decentralize and resource limited energy environments.

Upon discussing on technical part, it mostly focus on integrating the obtained bio-solar panel with an advance IoT-enabled real time monitoring system associated with sensors for measuring irradiance, temperature, voltage, uv-vis light , humidity, and thereby noticing panel health parameters as described in Fig.7 [38]. Real-time data obtained will be transmitted and stored to a cloud platform, where connection of AI and machine-learning models like CNN, deep learning, RNN algorithm can perform diagnostics, detection as early decay, and optimize panel performance operation through analytics and observations [39]. The combined proposal of bio-material and AI

framework can greatly evolve into a smart, advance and self-optimizing solar modules suitable for scalable rural and urban commercialization, facilitating improved dependability, efficiency forecasting, and at greater end term sustainability of bio- photovoltaic systems [40].

The present study successfully described that the application of artificial intelligence techniques for intelligent solar panel monitoring, energy prediction, anomaly detection, as well as surface image condition classification. Different machine learning were implemented and analyzed photovoltaic system behavior under varying environmental conditions.

For energy prediction, environmental parameters such as wind speed, sunshine duration, air pressure, solar radiation, air temperature, and relative humidity were optimized to forecast solar energy production. Multiple algorithms including Random Forest Regression, XG Boost, Cat Boost, and LSTM were identified. Among them, Random Forest Regression showed comparatively improvised predictive ability and effectively achieved the relationship between meteorological conditions as well as system production. The graphical analysis and examination metrics affirmed the practical reliability of Artificial intelligence based solar energy forecasting.

In the anomaly prediction module, parameters involving like irradiance, voltage, current, temperature, and power were estimation to identify abnormal operating parameters in the photovoltaic system. The deployed model demonstrated fault identification ability through confusion matrix analysis as well as classification performance. The obtained results explained the usefulness of AI-based predictive maintenance operations for improving solar panel consistency and operational efficiency.

Furthermore, a Convolutional Neural Network (CNN)-derived image classification model was integrating to classify solar panel surface situations into Clean, Dusty, and Snow-covered categories. The CNN model accomplished satisfactory performance with respect to the validation accuracy reaching for about 78–82% after many training epochs. Accuracy curves, loss curves, confusion matrices, as well as classification reports appraised that the model successfully get trained meaningful image features and thereby performed automated conditions classification with effect.

Although, the integration of machine learning and computer vision techniques defined significant potential for decremention of intelligent and automated solar motorization. The proposed framework can hold up efficient photovoltaic performance detection, early fault monitoring, and smart energy management in energy applications.

turnitin Page 42 of 43 - Integrity Submission Submission ID trn:oid:::1:3579406073

turnitin Page 43 of 43 - Integrity Submission Submission ID trn:oid:::1:3579406073